Table 4.1 The effects of the disk rotation on the critical condition for appearance of the inertia-driven vortex roll (ΔT= 0℃, H=20.0 mm and D_j=10.0 mm).

Vortex Roll	Disk rotation speed (Ω, rpm)	Flowrate (Q_j, SLPM)	Re_Ω	Re_j
Primary inertia-driven roll	0	0.1	0	14
	5	0.2	389	27
	10	0.3	778	41
	15	0.4	1,168	54
Secondary inertia-driven roll	0	1.3	0	180
	5	1.4	389	190
	10	1.6	778	216
	15	1.9	1,168	257
Tertiary inertia-driven roll	0	5.0	0	676
	10	5.0	778	676
	15	5.3	1,168	717
	20	5.8	1,557	784

Table 4.2 The effects of the disk rotation on the critical condition for onset of the buoyancy-driven vortex flow (H=20.0 mm and D_j=10.0 mm).

Disk rotation speed (Ω, rpm)	Flowrate (Q_j, SLPM)	Temperature difference ΔT(℃)	Re_j	Gr	Ra	Gr/Re_j^2
$Re_\Omega = 0$ ($\Omega = 0$ rpm)	5.5	2.2	744	2,362	1,654	0.0043
	7.2	4.0	974	4,295	3,007	0.0045
	9.4	7.0	1,271	7,516	5,621	0.0046
	11.4	10.0	1,542	10,737	7,516	0.0045
$Re_\Omega = 389$ ($\Omega = 5$ rpm)	5.5	6.4	744	6,872	4,810	0.0118
	7.2	10.1	974	10,845	7,590	0.0115
	9.4	17.4	1,271	13,530	9,470	0.0116
	11.4	25.3	1,542	27,165	19,016	0.0114
$Re_\Omega = 778$ ($\Omega = 10$ rpm)	5.5	12.1	744	12,990	9,095	0.0235
	7.2	20.5	974	22,012	15,408	0.0232
	9.4	34.8	1,271	37,370	26,160	0.0232
	11.4	51.6	1,542	55,405	38,785	0.0233

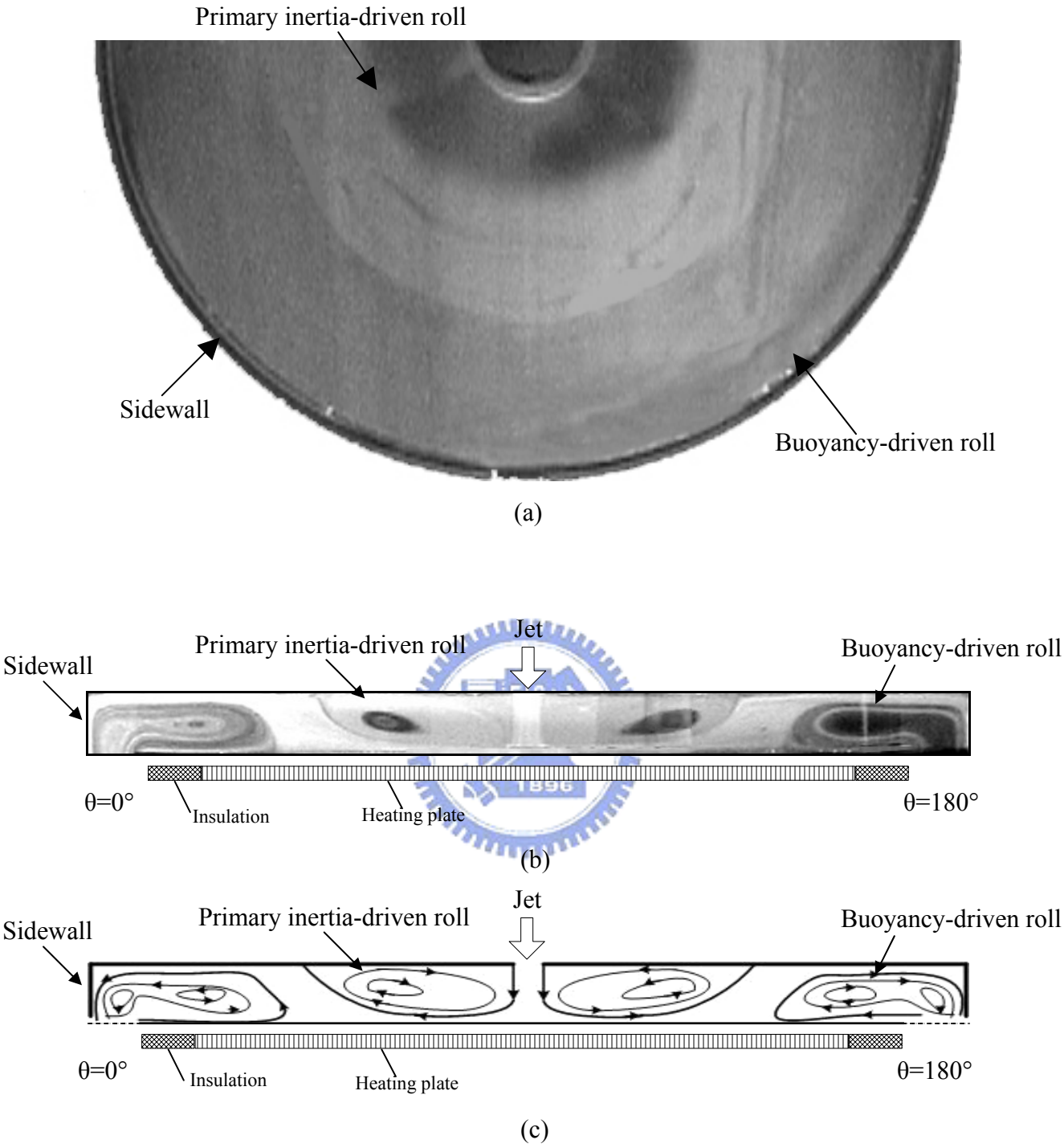

Fig. 4.1 Steady vortex flow pattern in the chamber with D_j = 10.0 mm and H=20.0 mm for Re_j = 270 (Q_j = 2.0 slpm), Ra = 15,030 (ΔT = 20.0°C) and Re_Ω = 0 (Ω = 0 rpm): (a) top view flow photo taken at middle horizontal plane halfway between the pipe exit and heated disk, (b) side view flow photo taken at the vertical plane $\theta = 0^\circ$ & 180°, and (c) the corresponding schematically sketched cross plane vortex flow.

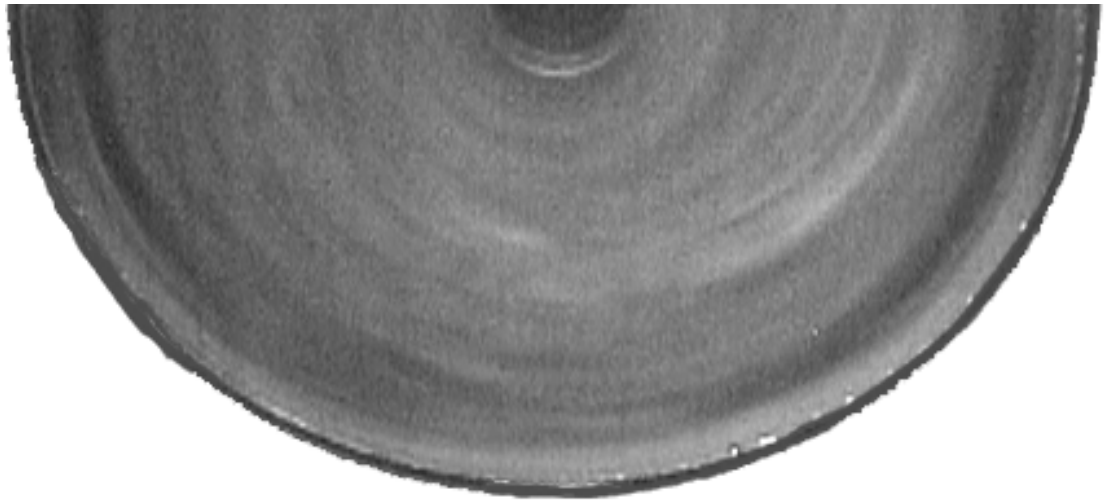

(a) steady state

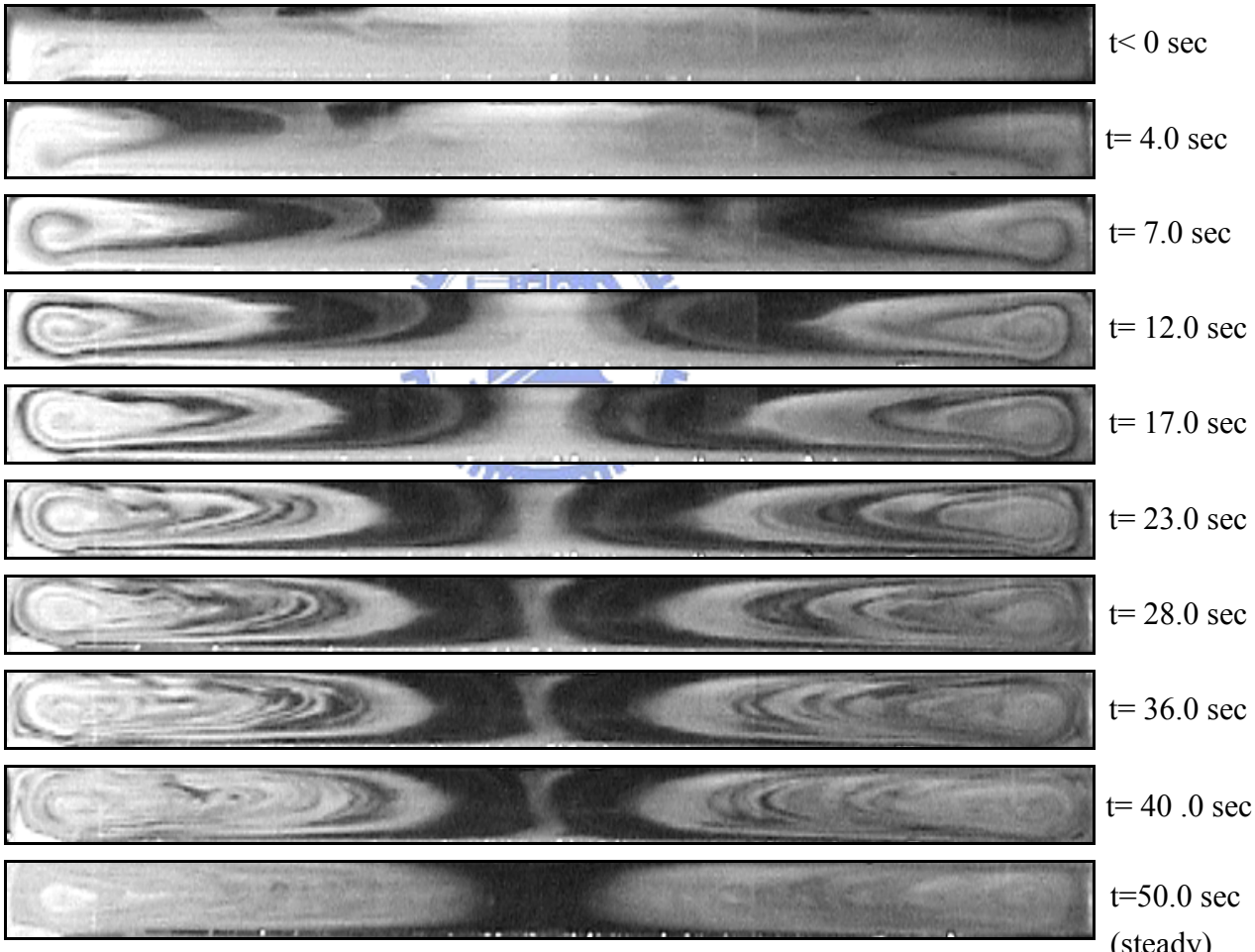

(b)

Fig. 4.2 Vortex flow formation for D_j = 10.0 mm and H=20.0 mm at Re_j = 0, Ra = 0 and Re_Ω = 778 (Ω = 10 rpm): (a) top view flow photo taken at the middle horizontal plane between the disk and chamber top, and (b) side view flow photo taken at the vertical plane $\theta = 0^\circ$ & 180°.

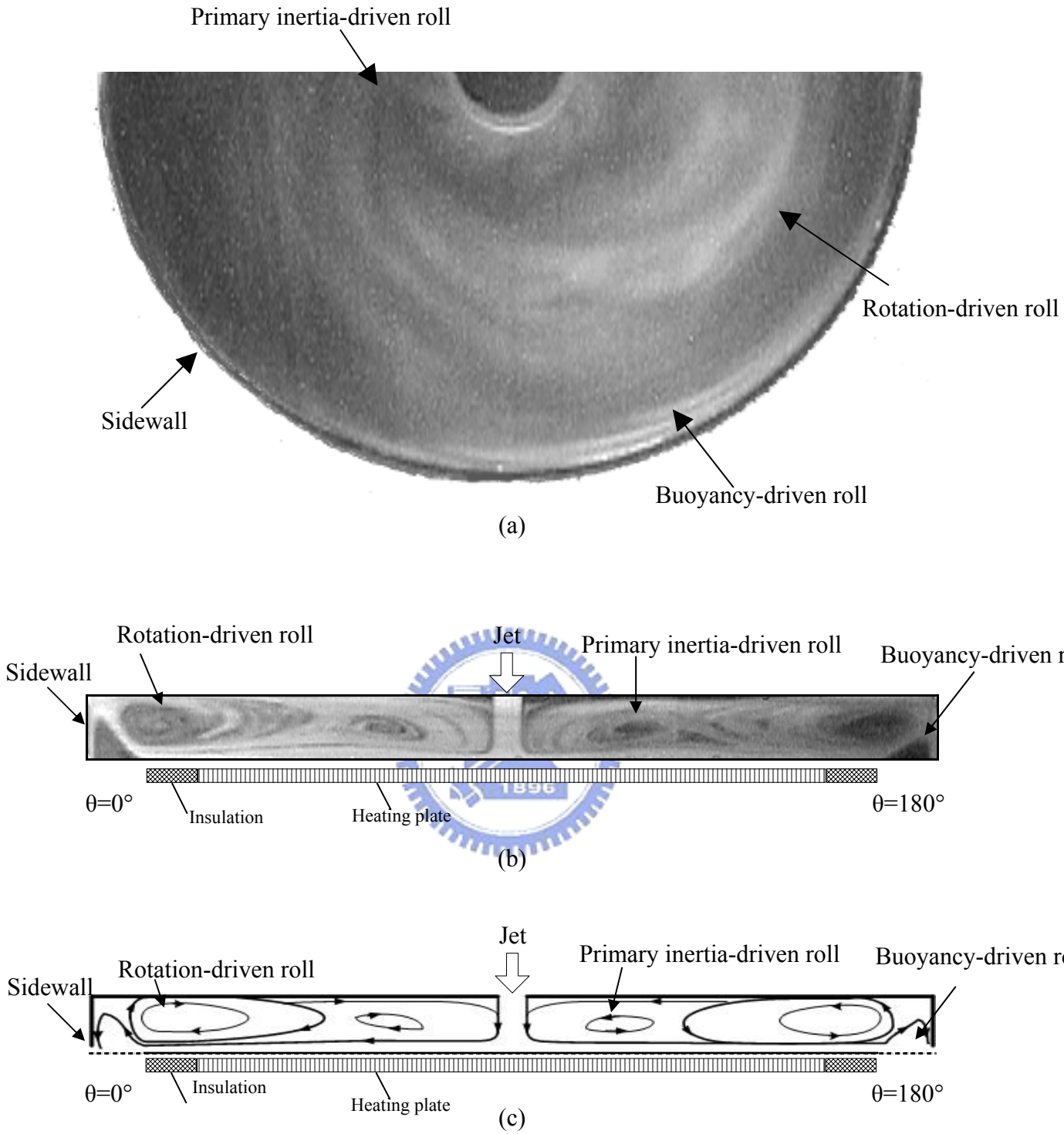

Fig. 4.3 Steady vortex flow pattern for D_j = 10.0 mm and H=20.0 mm at Re_j = 270 (Q_j = 2.0 slpm), Ra = 15,030 (ΔT = 20.0℃) and Re_Ω = 2,335 (Ω = 30 rpm): (a) top view flow photo taken at the middle horizontal plane between the disk and chamber top, (b) side view flow photo taken at the vertical plane $\theta = 0^\circ$ & 180°, and (c) the corresponding schematically sketched cross plane vortex flow.

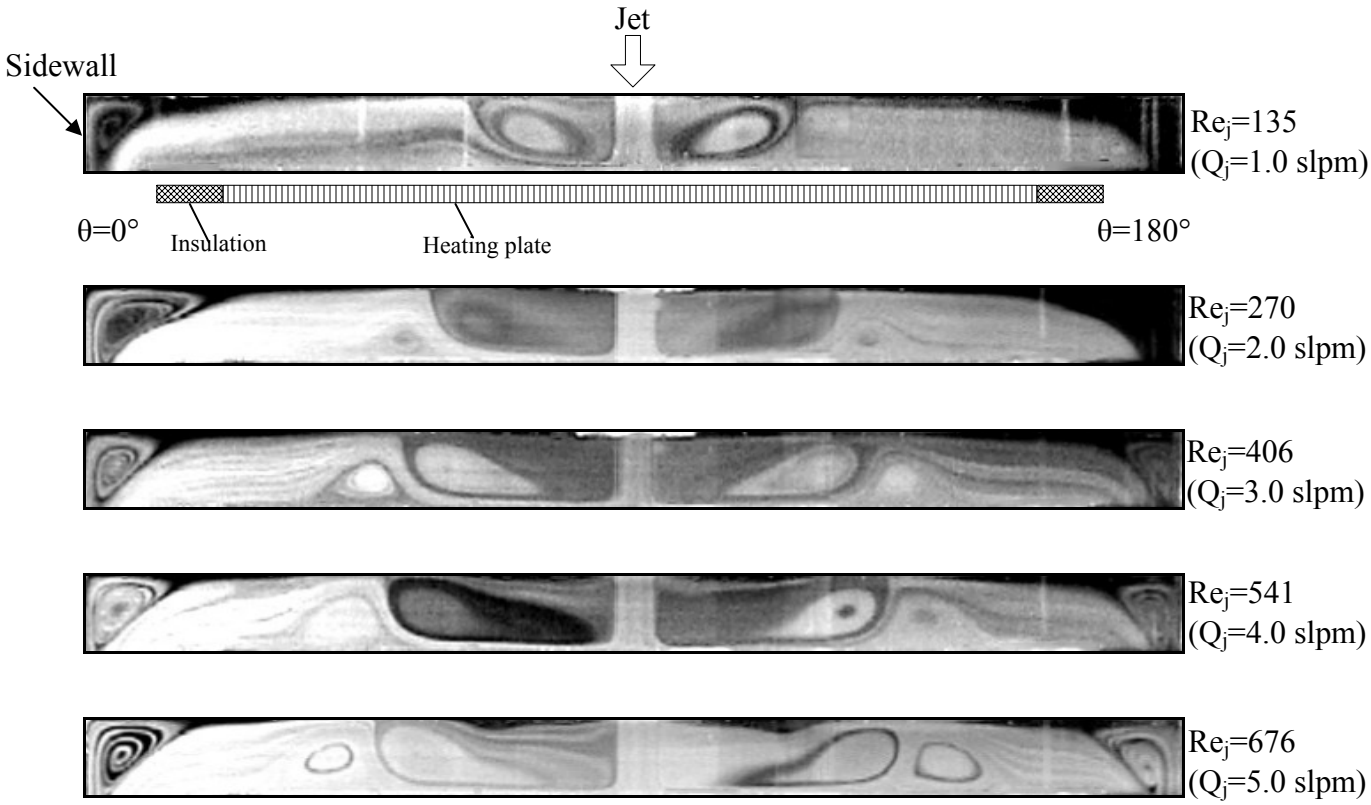

(a) D_j=10.0 mm

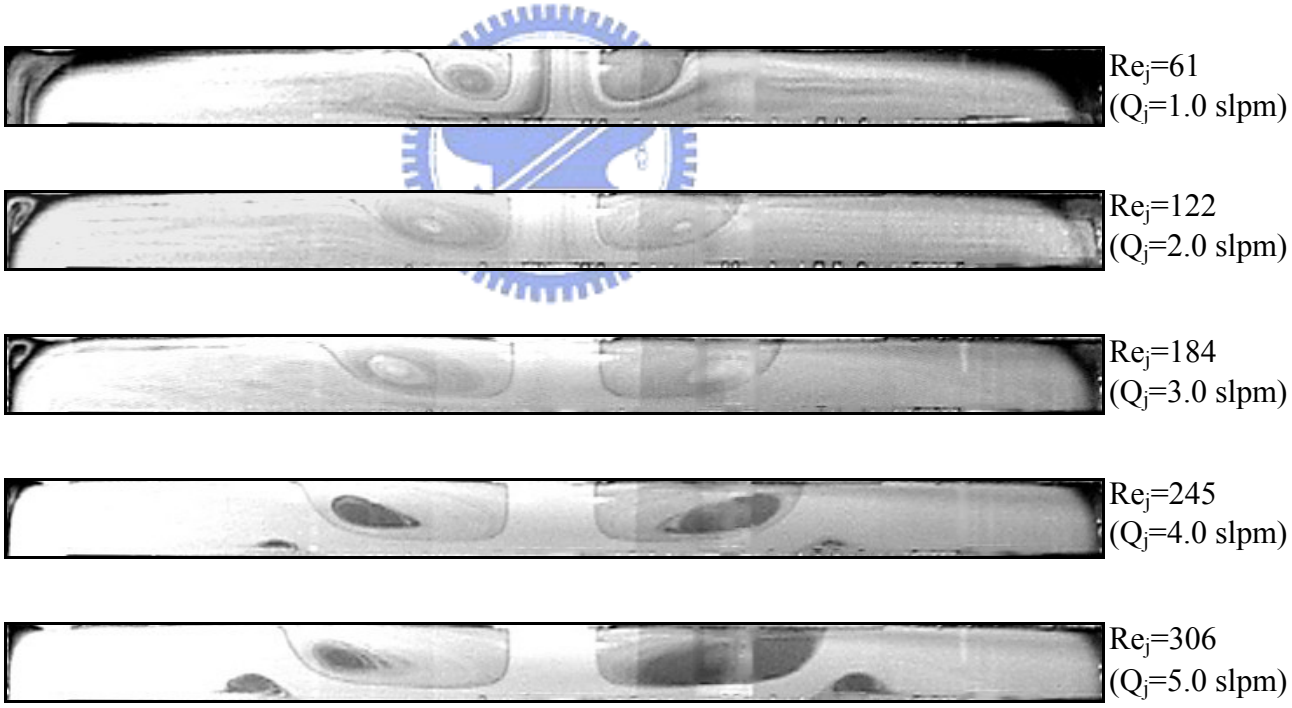

(b) D_j=22.1 mm

Fig. 4.4 Steady side view flow photos taken at the cross plane $\theta = 0^\circ$ & 180° for various jet Reynolds numbers at Ra = 0 ($\Delta T = 0^\circ C$) and $Re_\Omega = 0$ ($\Omega = 0$ rpm) for D_j = (a) 10.0 mm and (b) 22.1 mm.

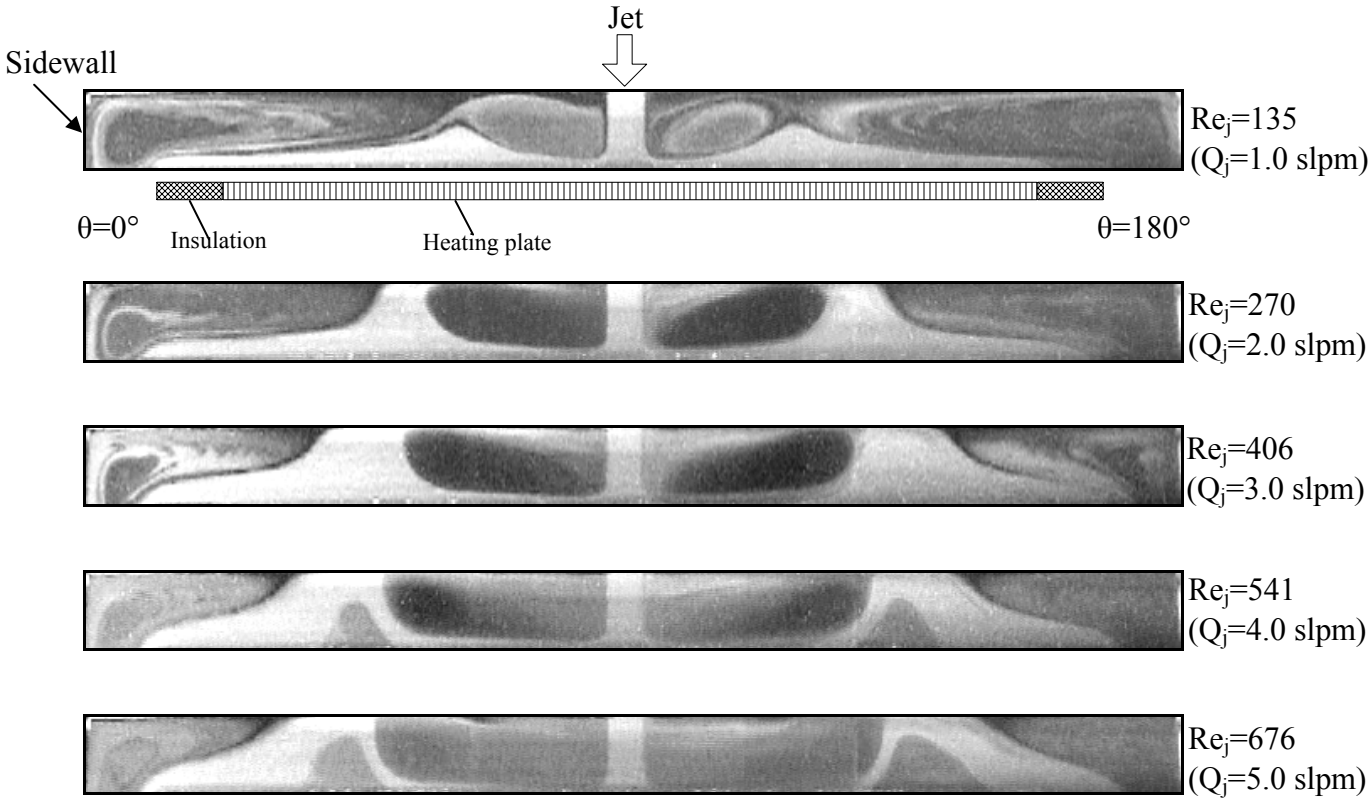

(a) D_j=10.0 mm

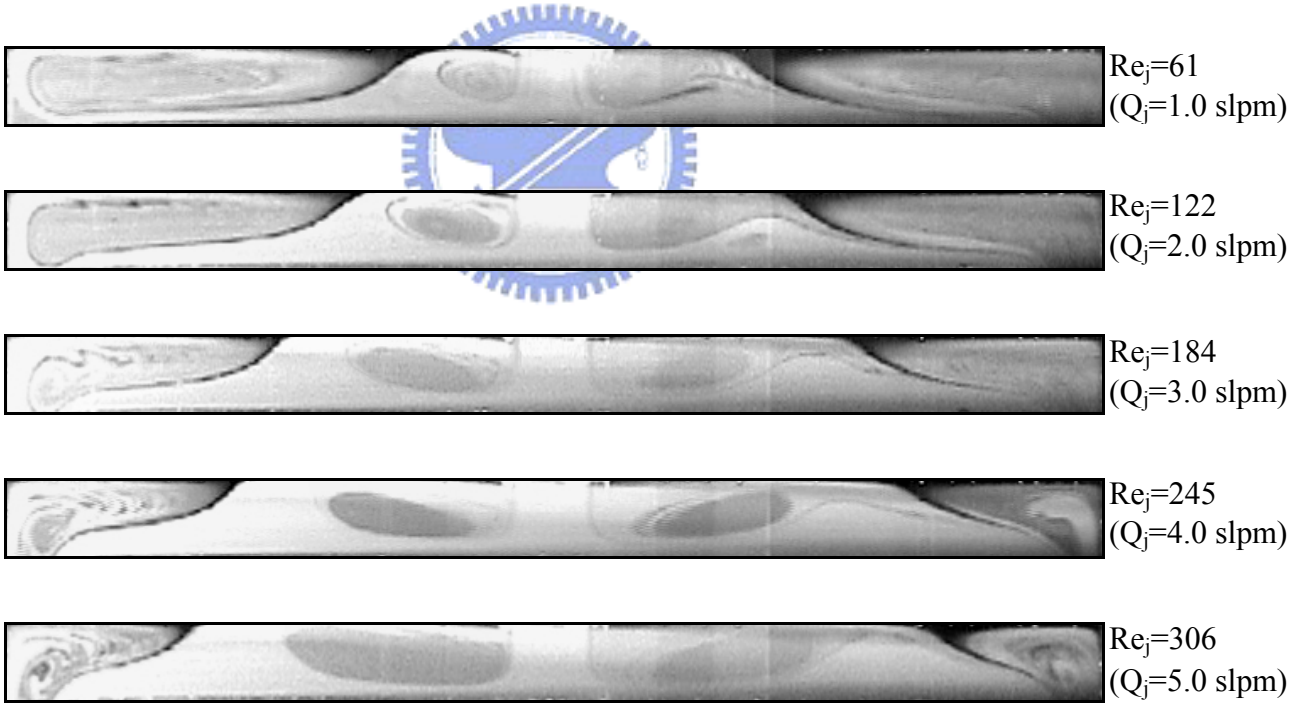

(b) D_j=22.1 mm

Fig. 4.5 Steady side view flow photos taken at the cross plane $\theta = 0^\circ$ & 180° for various jet Reynolds numbers at Ra = 0 ($\Delta T = 0^\circ C$) and $Re_\Omega = 778$ ($\Omega = 10$ rpm) for D_j = (a) 10.0 mm and (b) 22.1 mm.

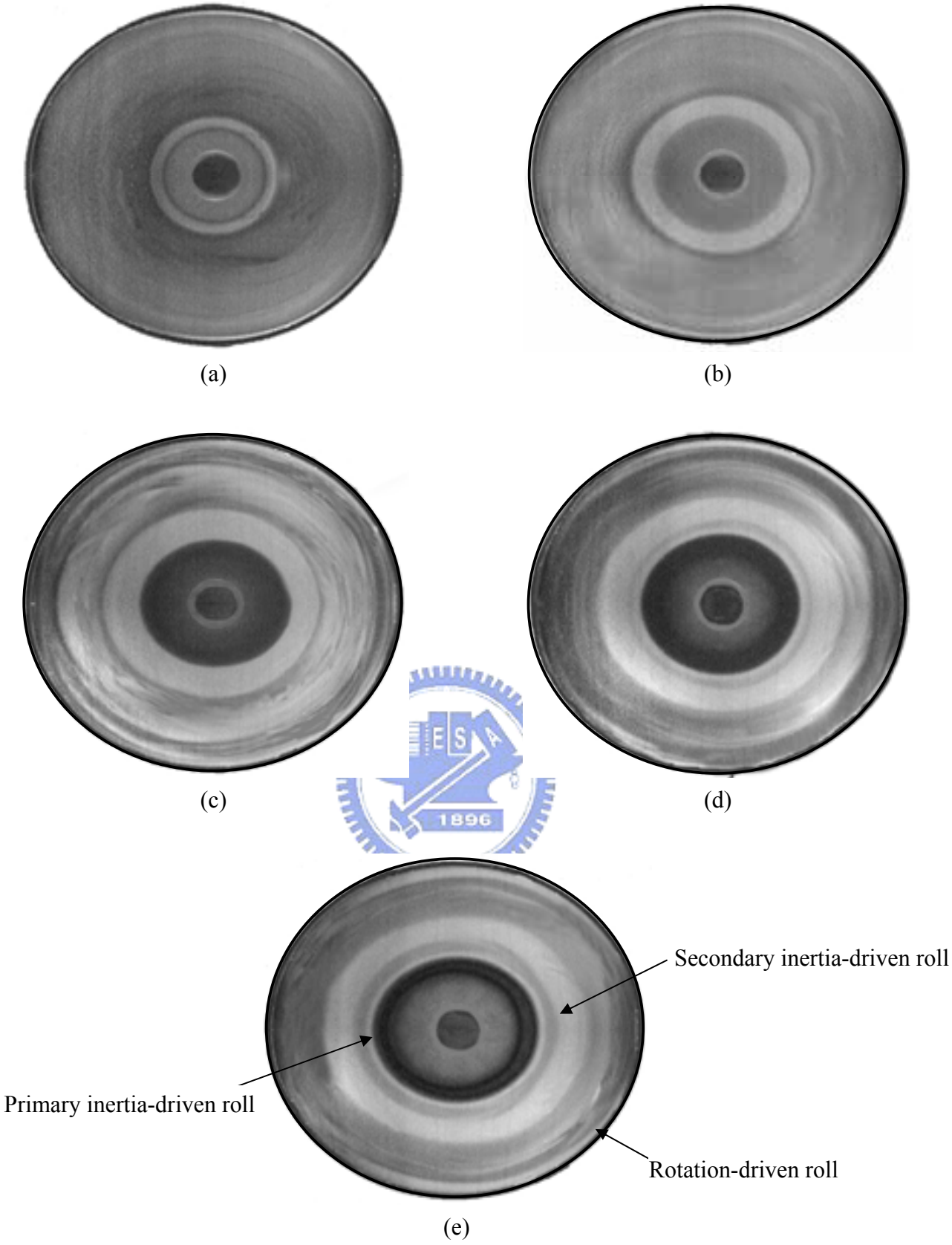

Fig. 4.6 Top view flow photos taken at the middle horizontal plane between the disk and chamber top with Ra = 0 ($\Delta T = 0^{\circ}C$), $Re_{\Omega} = 778$ ($\Omega = 10$ rpm) and $D_j = 10.0$ mm for $Re_j =$ (a) 135, (b) 270, (c) 406, (d) 541, and (e) 676.

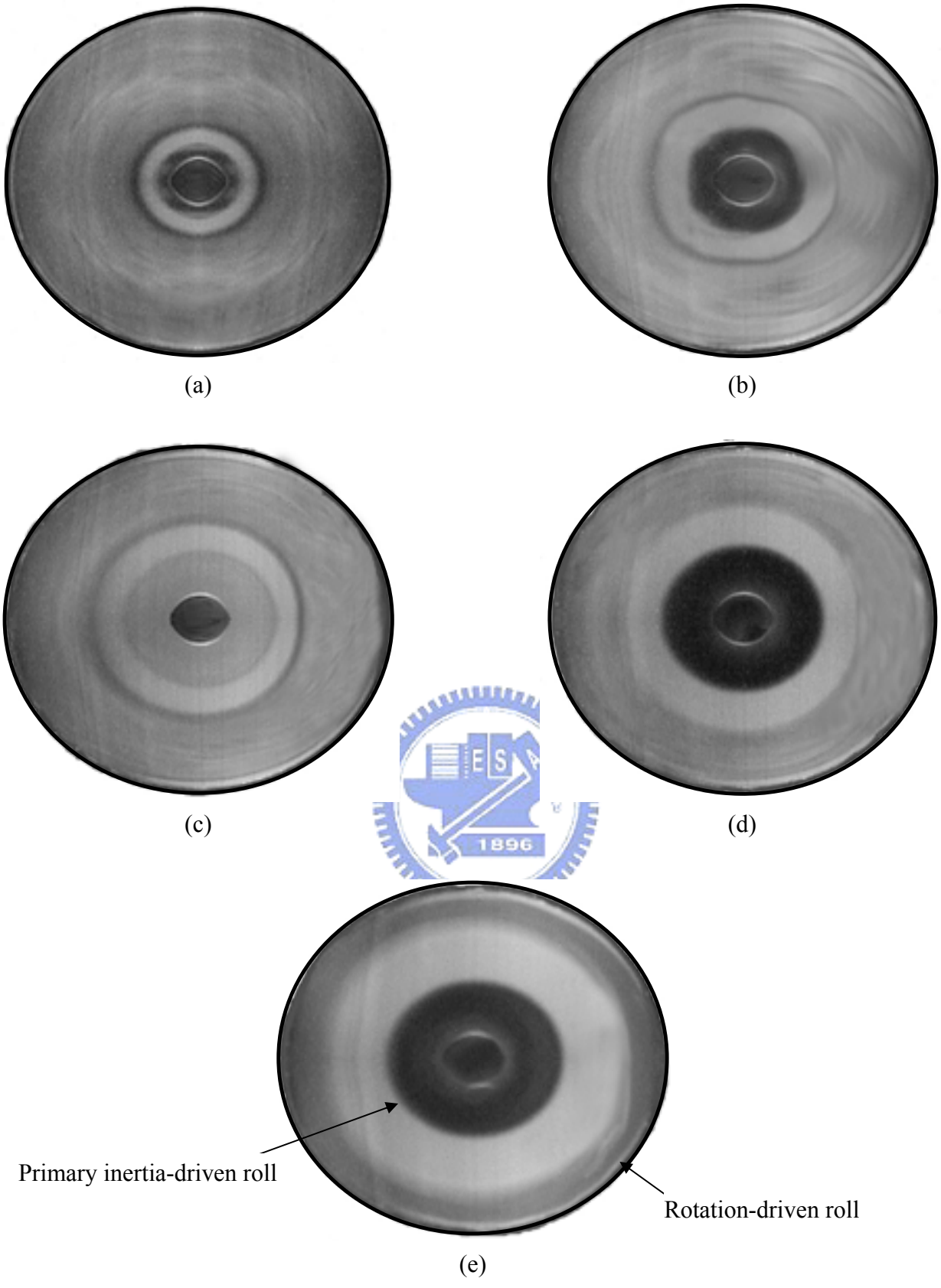

Fig. 4.7 Top view flow photos taken at the middle horizontal plane between the disk and chamber top with Ra = 0 ($\Delta T = 0^{\circ}C$), $Re_{\Omega} = 778$ ($\Omega = 10$ rpm) and $D_j = 22.1$ mm for $Re_j =$ (a) 61, (b) 122, (c) 184, (d) 245, and (e) 306.

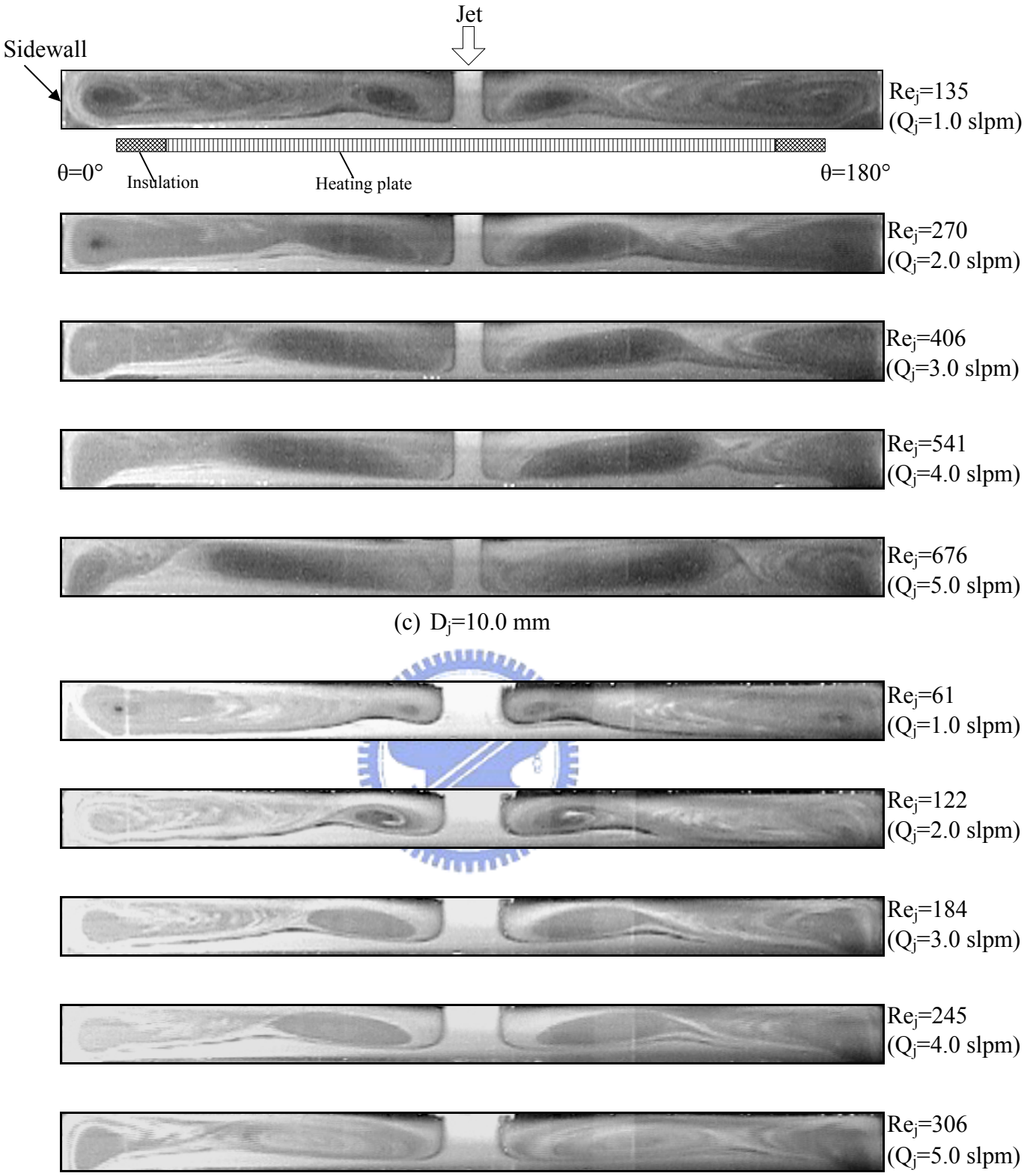

Fig. 4.8 Steady side view flow photos taken at the cross plane $\theta = 0^\circ$ & 180° for various jet Reynolds numbers at Ra = 0 ($\Delta T = 0^\circ C$) and $Re_\Omega = 1{,}557$ ($\Omega = 20$ rpm) for D_j = (a) 10.0 mm and (b) 22.1 mm.

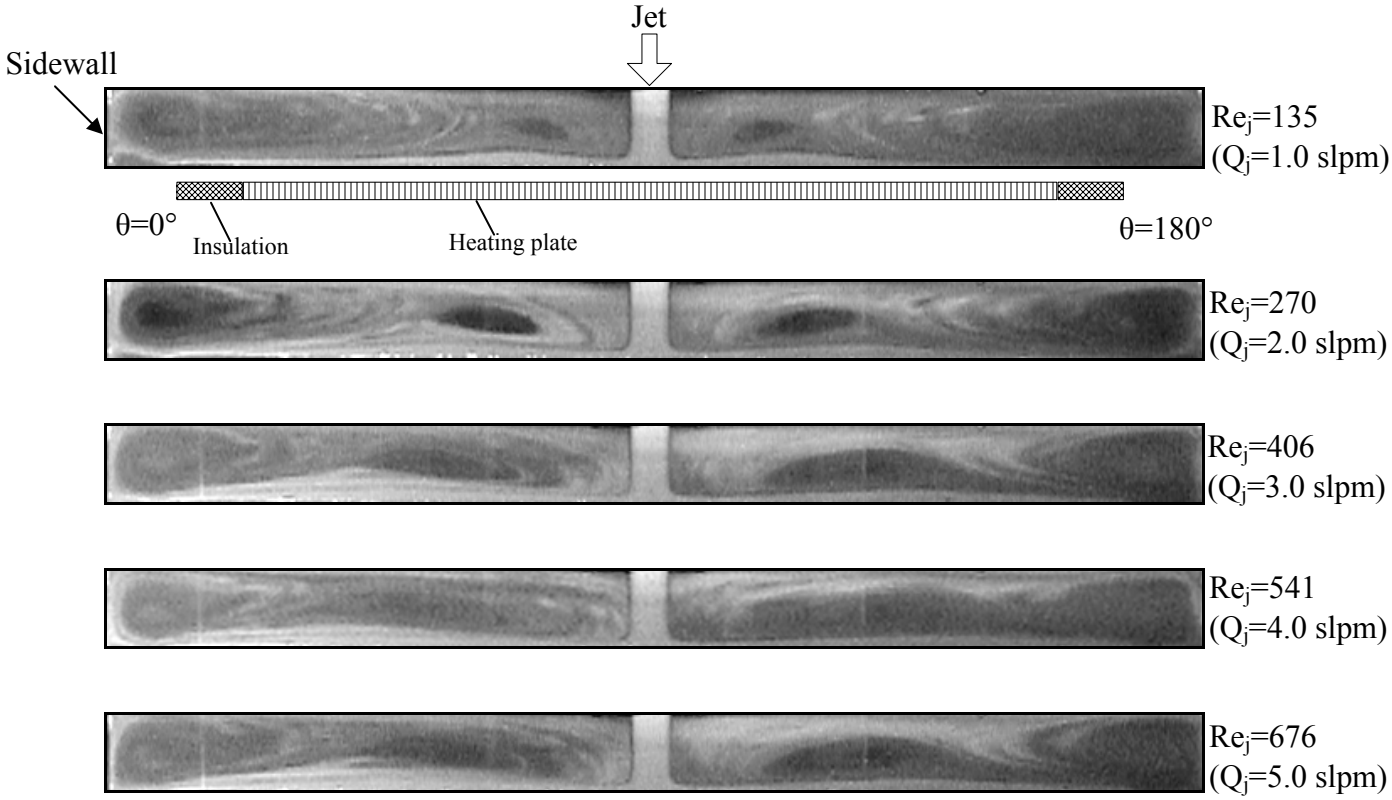

(a) D_j=10.0 mm

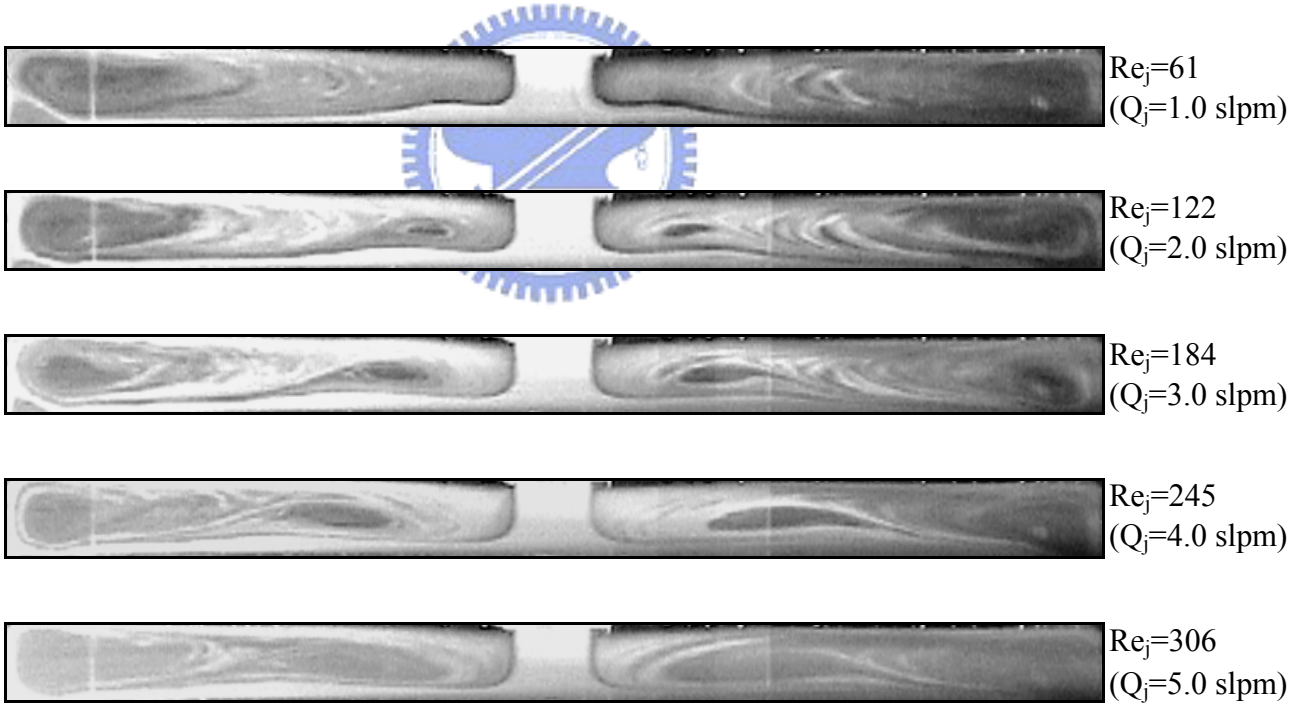

(b) D_j=22.1 mm

Fig. 4.9 Steady side view flow photos taken at the cross plane $\theta = 0^\circ$ & 180° for various jet Reynolds numbers at Ra = 0 ($\Delta T = 0^\circ C$) and $Re_\Omega = 2{,}335$ ($\Omega = 30$ rpm) for D_j = (a) 10.0 mm and (b) 22.1 mm.

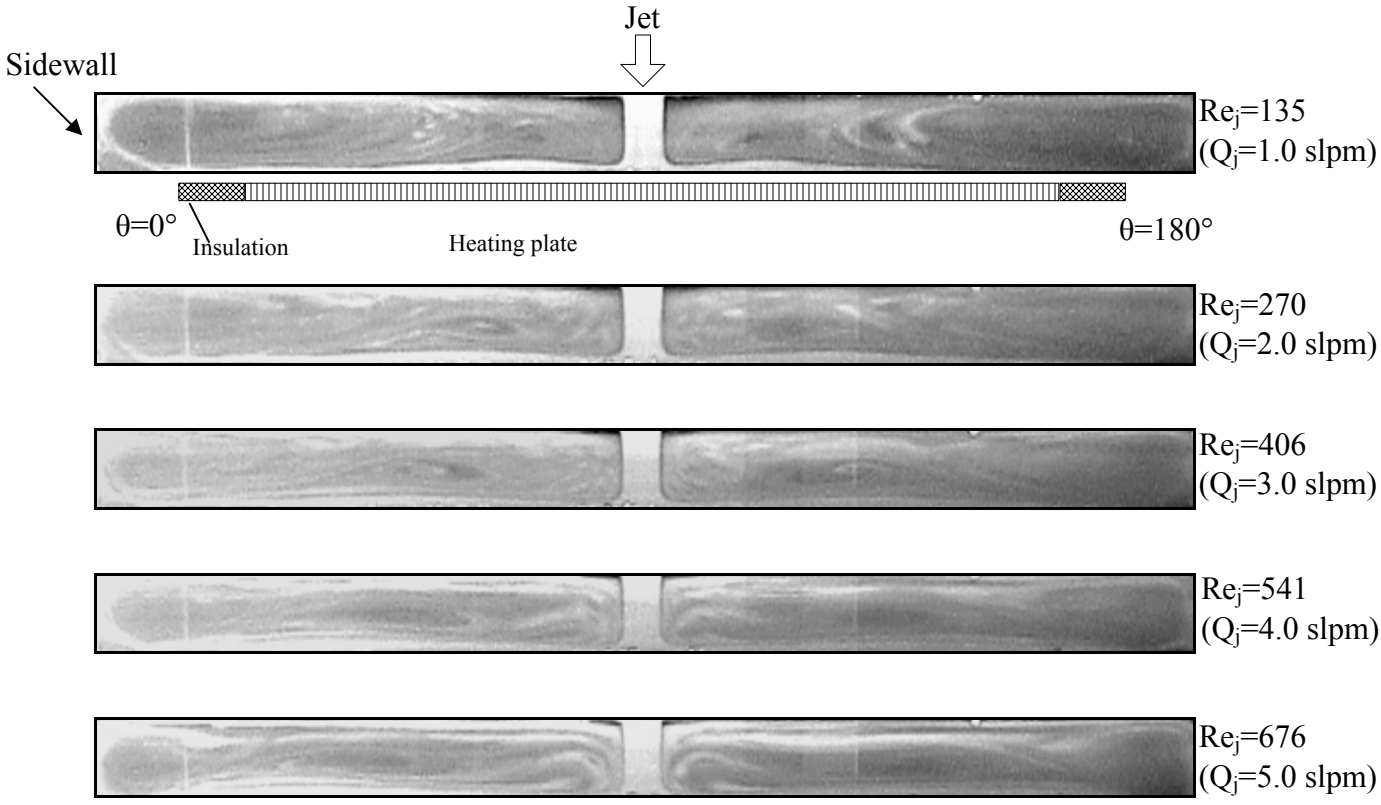

(b) D_j=10.0 mm

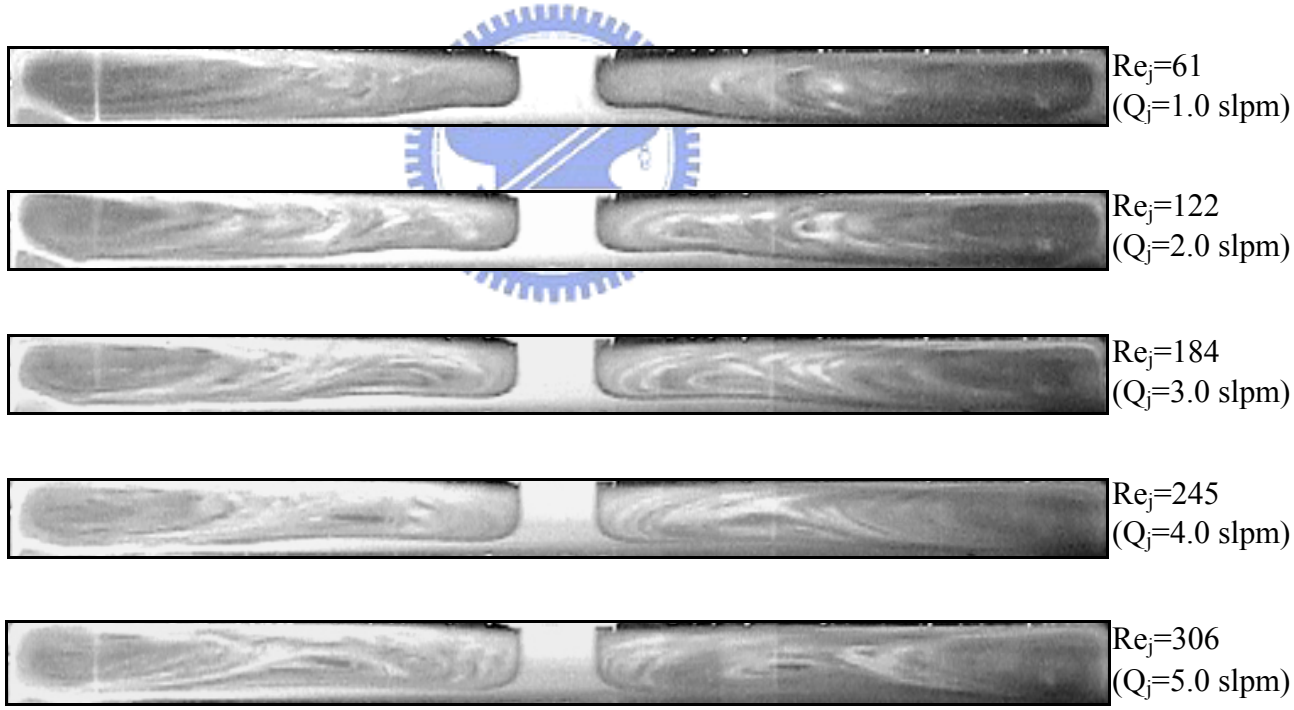

(b) D_j=22.1 mm

Fig. 4.10 Steady side view flow photos taken at the cross plane $\theta = 0^\circ$ & 180° for various jet Reynolds numbers at Ra = 0 ($\Delta T = 0^\circ C$) and Re_Ω = 3,114 (Ω = 40 rpm) for D_j = (a) 10.0 mm and (b) 22.1 mm.

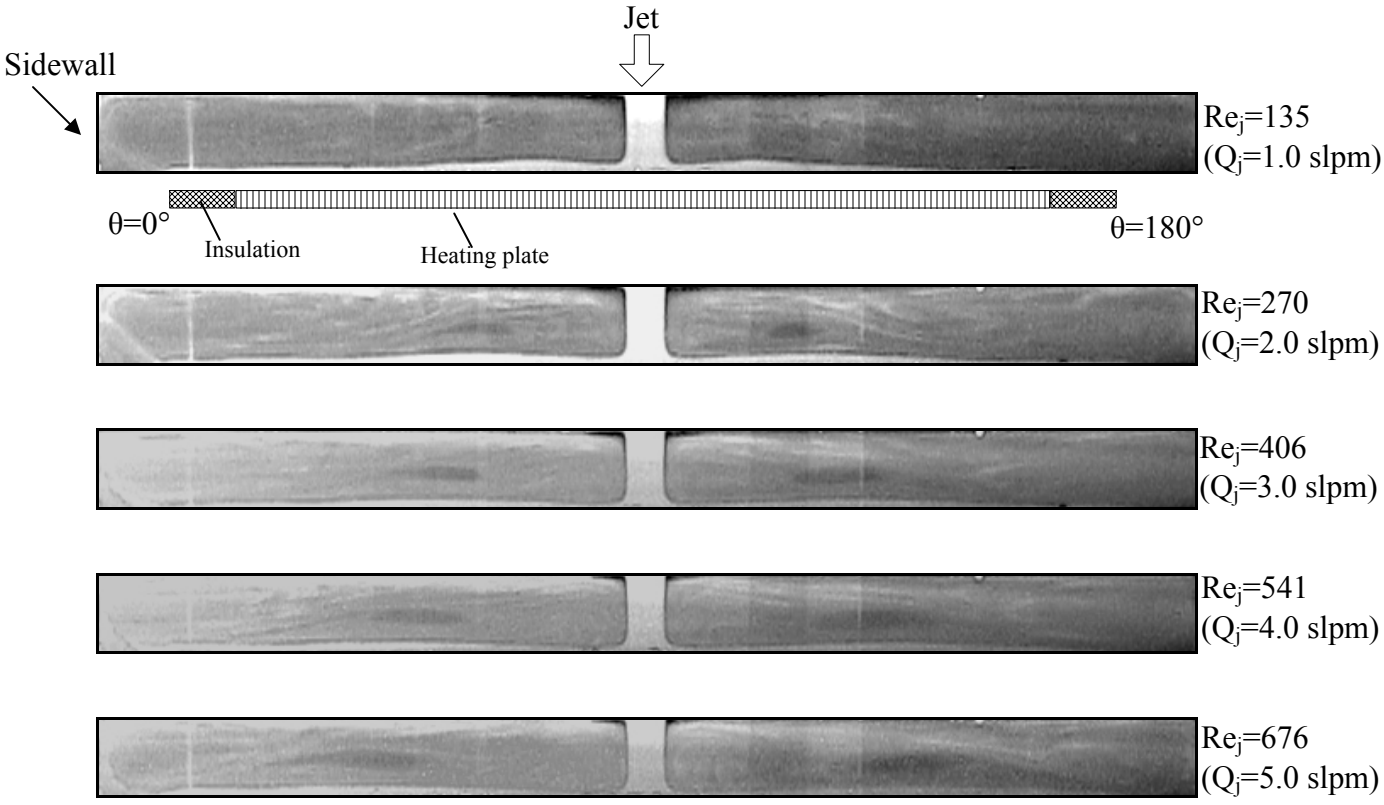

(a) D_j=10.0 mm

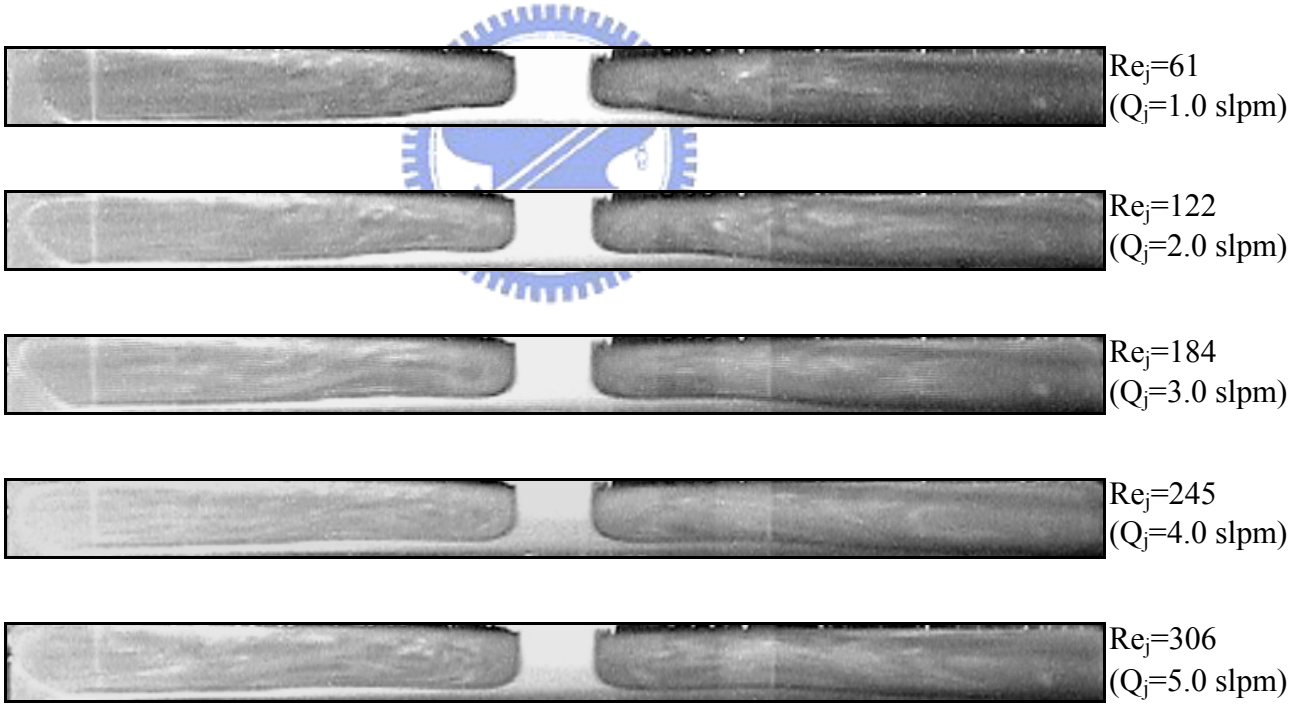

(b) D_j=22.1 mm

Fig. 4.11 Steady side view flow photos taken at the cross plane $\theta = 0^\circ$ & 180° for various jet Reynolds numbers at Ra = 0 ($\Delta T = 0^\circ C$) and Re_Ω = 3,892 (Ω = 50 rpm) for D_j = (a) 10.0 mm and (b) 22.1 mm.

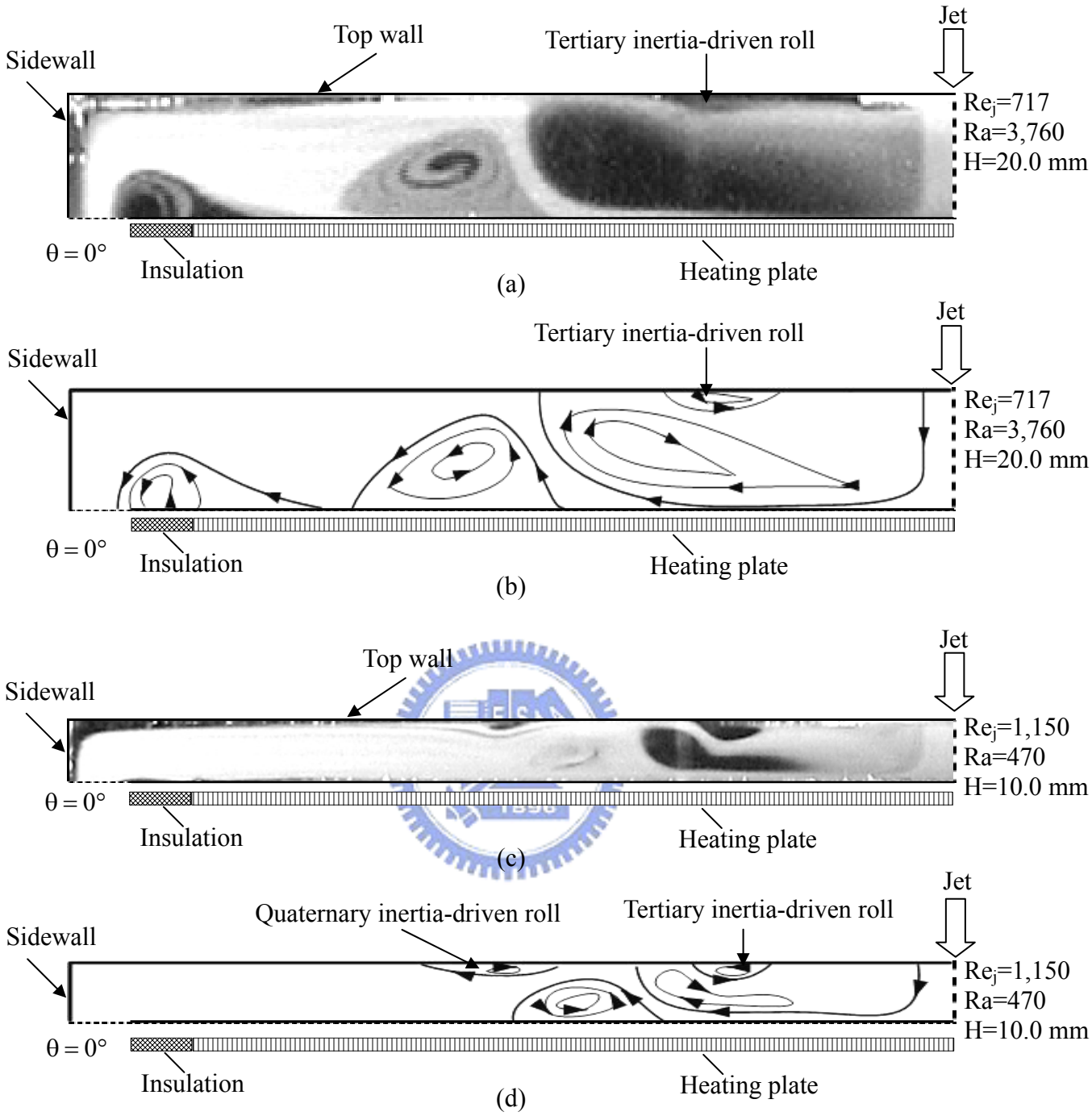

Fig. 4.12 Steady vortex flow pattern in the chamber with D_j=10.0 mm: (a) side view flow photo taken at the vertical plane $\theta = 0^\circ$ for H=20.0 mm at Re_j=717 (Q_j=5.3 slpm) and Ra=3,760 ($\Delta T = 5.0$ ℃) and (b) the corresponding schematically sketched cross plane vortex flow, and (c) side view flow photo for H=10.0 mm at Re_j=1,150 (Q_j=8.5 slpm) and Ra=470 ($\Delta T = 5.0$ ℃) and (d) the corresponding schematically sketched cross plane vortex flow.

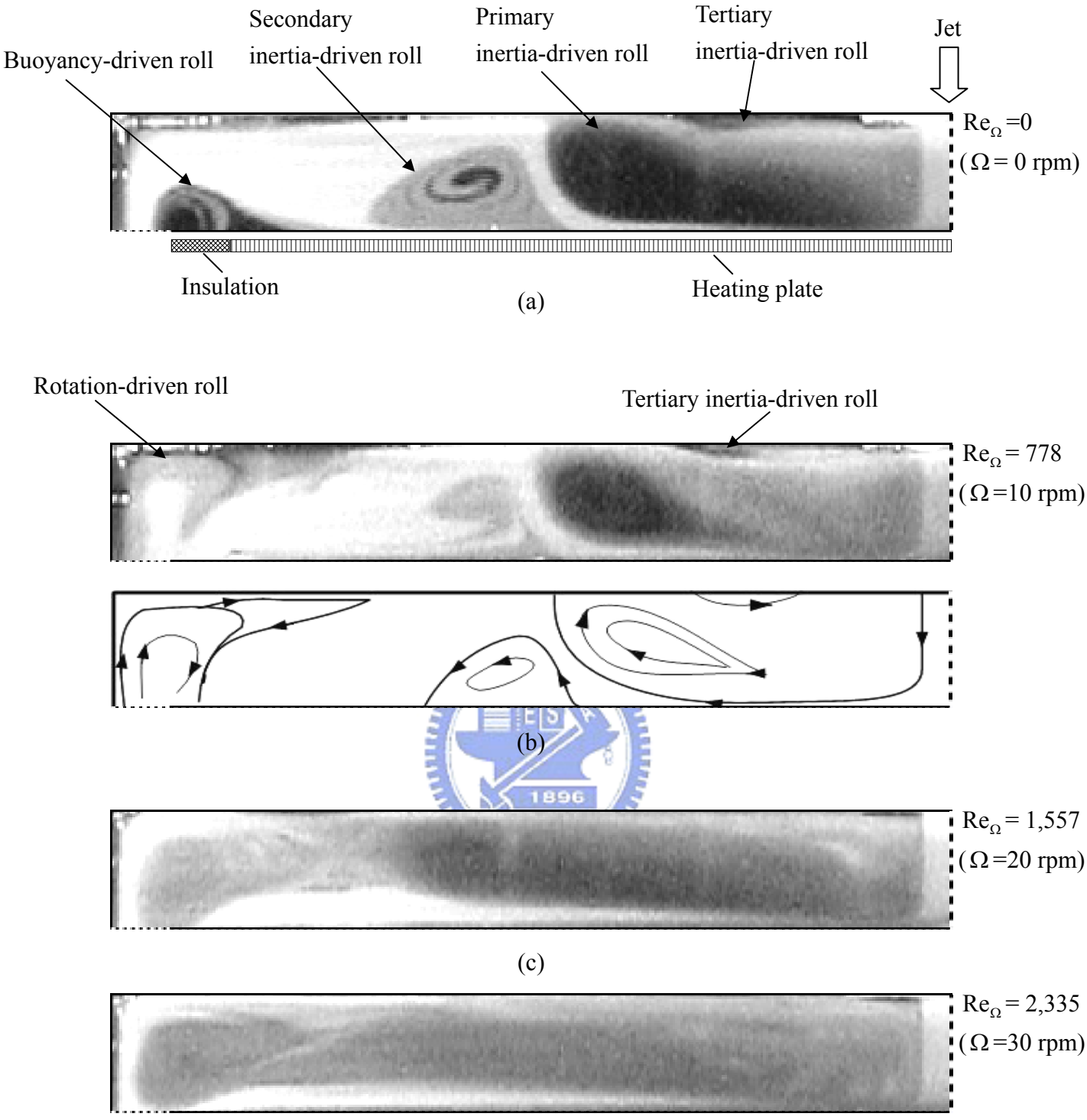

Fig. 4.13 Steady side view flow photos taken at the cross plane $\theta = 0°$ at H=20.0 mm for Ra=3,760 (ΔT = 5.0℃) and Re_j= 717 (Q_j=5.3 slpm) for rotational Reynolds number Re_Ω = (a)0, (b)778, (c)1,557, and (d)2,335.

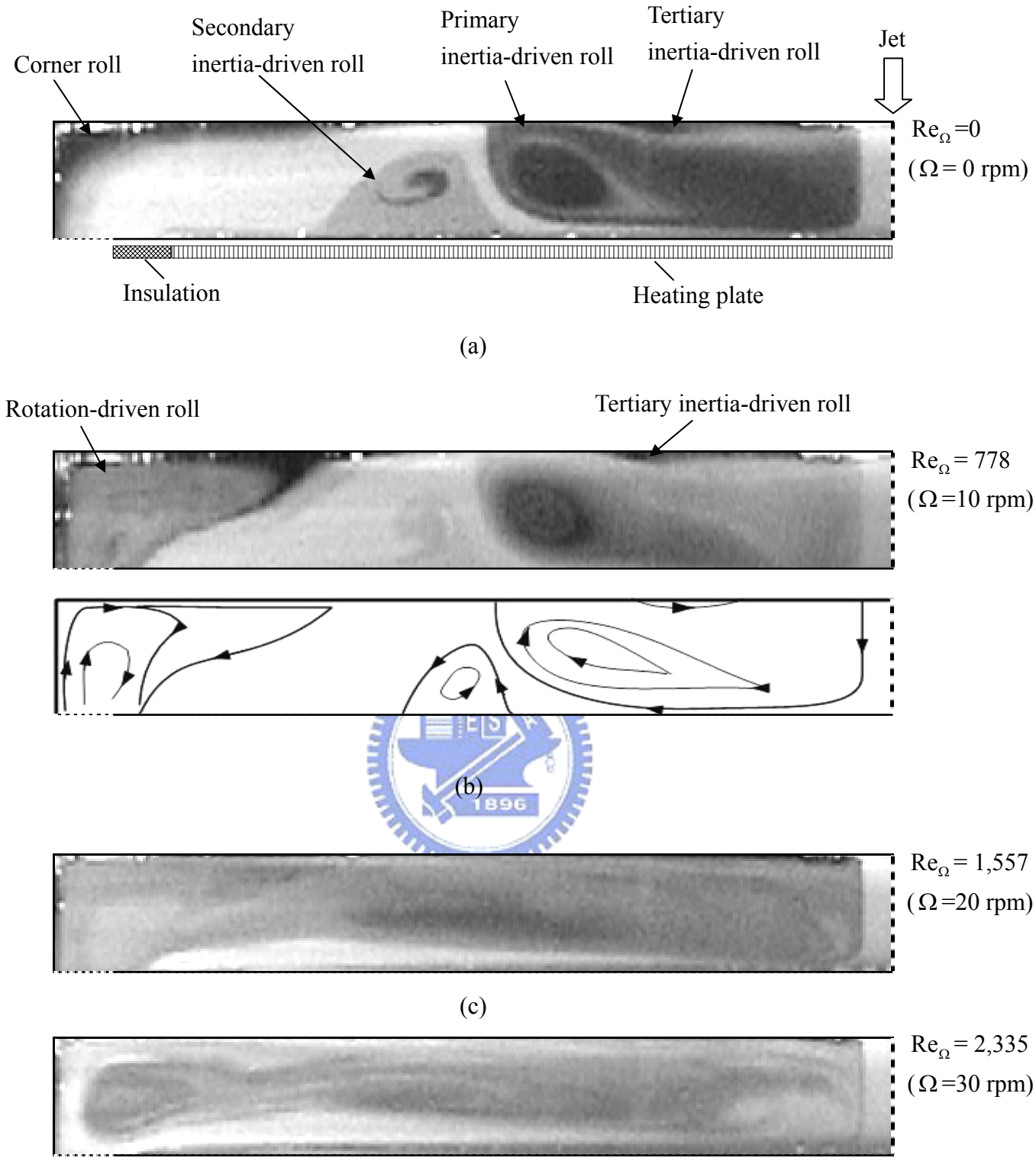

Fig. 4.14 Steady side view flow photos taken at the cross plane $\theta = 0°$ at H=20.0 mm for Ra=0 ($\Delta T = 0°C$) and Re_j= 676 (Q_j=5.0 slpm) for rotational Reynolds number Re_Ω = (a)0, (b)778, (c)1,557, and (d)2,335.

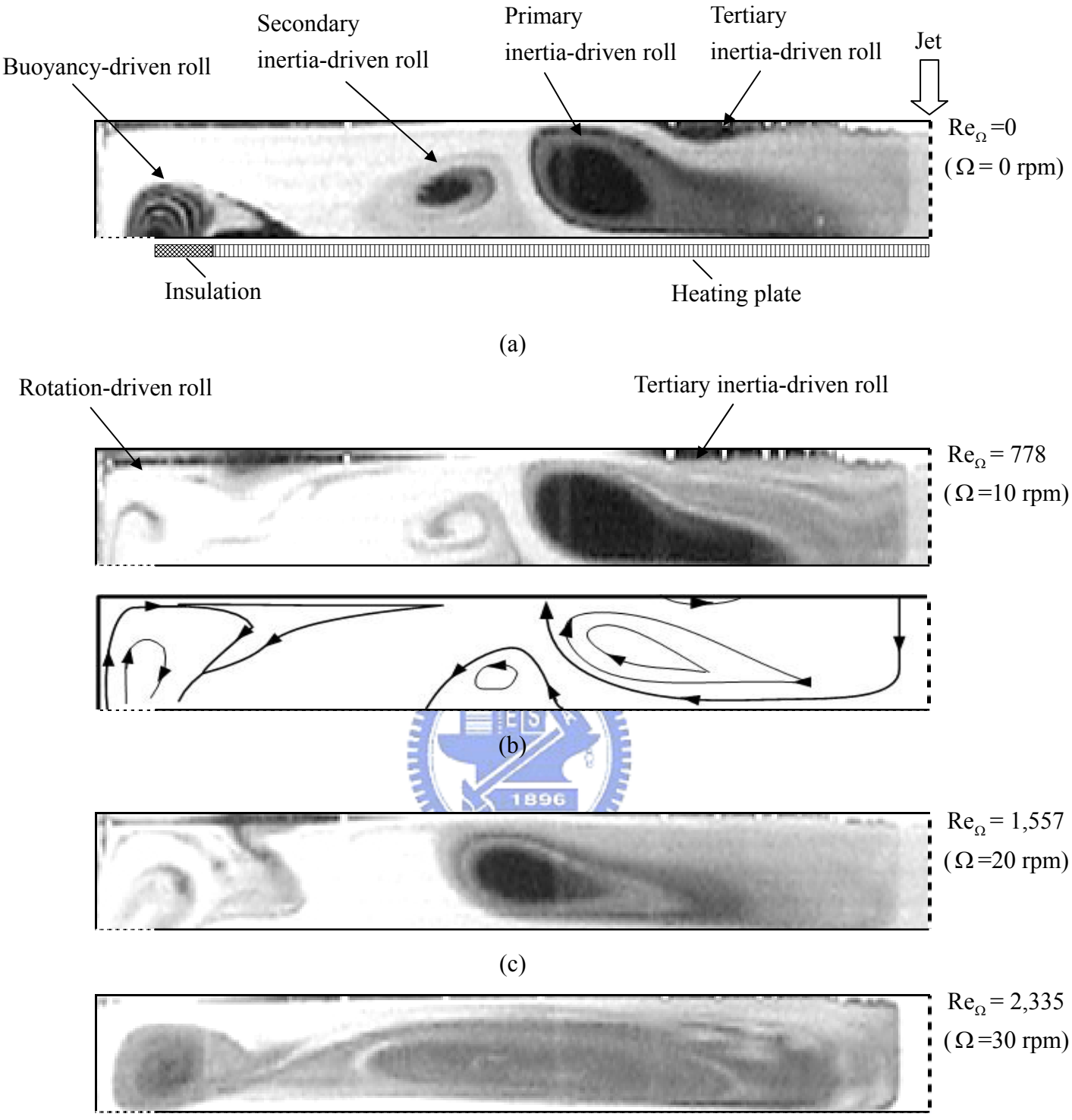

Fig. 4.15 Steady side view flow photos taken at the cross plane $\theta = 0°$ at H=20.0 mm for Ra=7,520 (ΔT =10.0℃) and Re_j= 730 (Q_j=5.4 slpm) for rotational Reynolds number Re_Ω = (a)0, (b)778, (c)1,557, and (d)2,335.

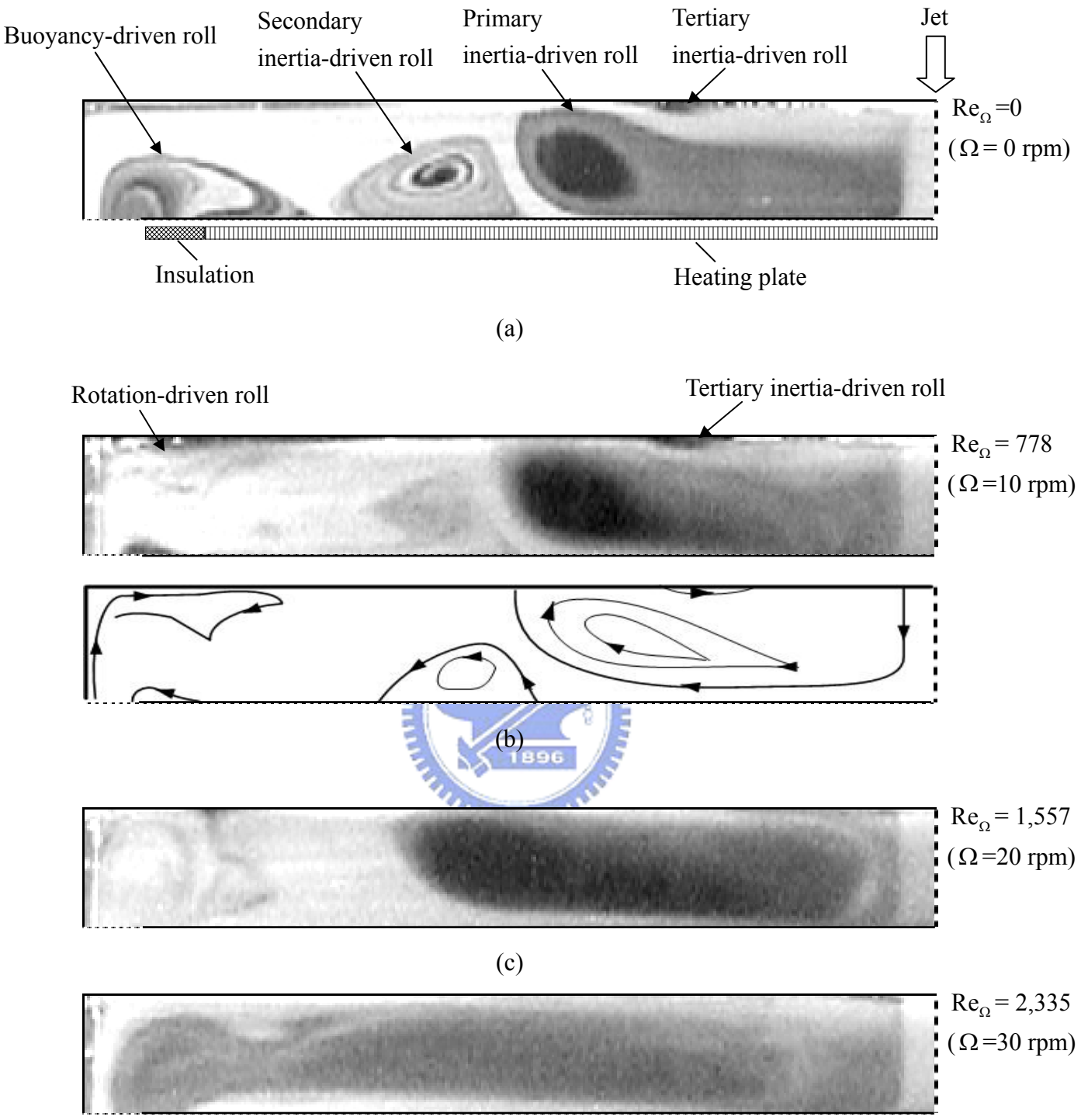

Fig. 4.16 Steady side view flow photos taken at the cross plane $\theta = 0°$ at H=20.0 mm for Ra=11,270 (ΔT =15.0℃) and Re_j= 771 (Q_j=5.7 slpm) for rotational Reynolds number Re_Ω = (a)0, (b)778, (c)1,557, and (d)2,335.

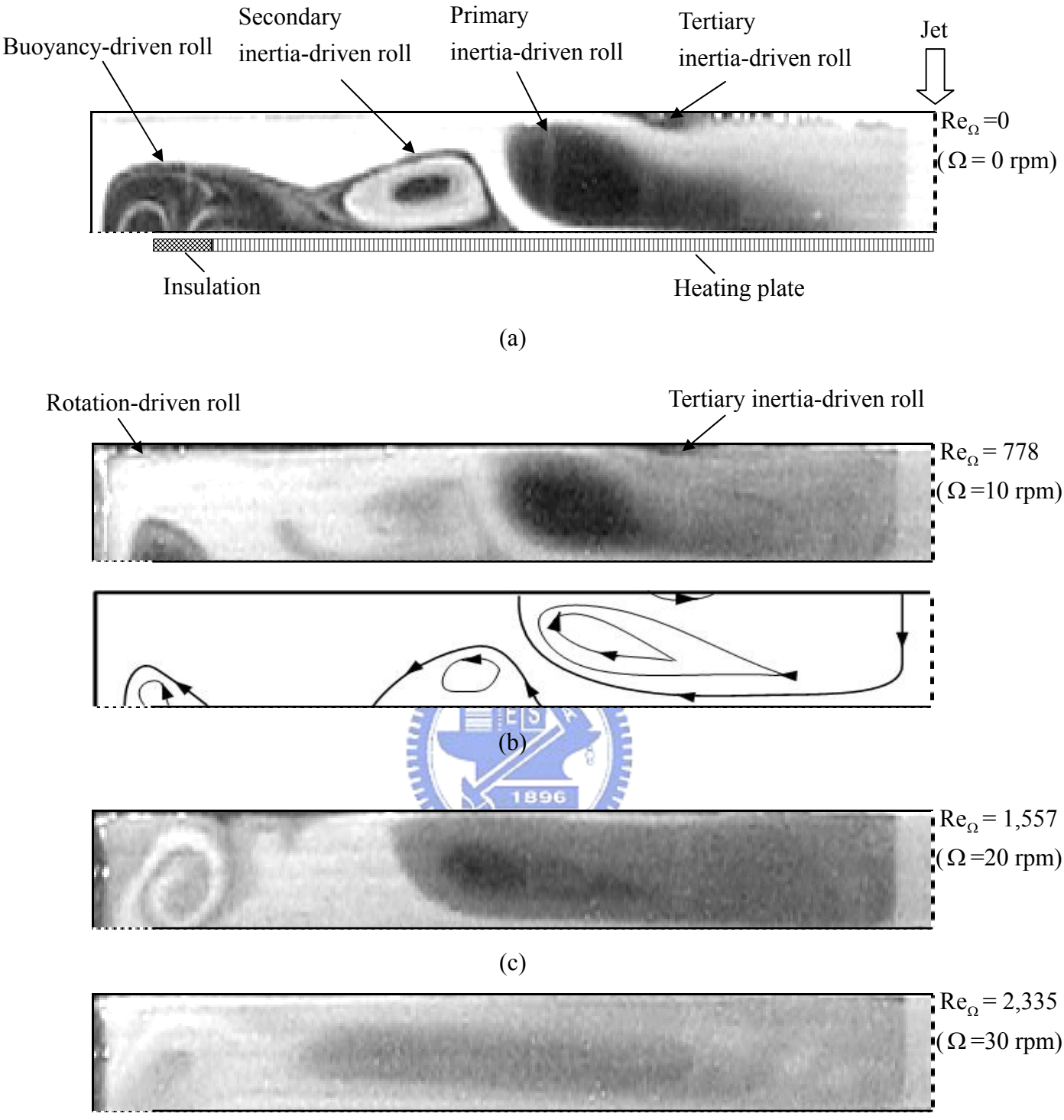

Fig. 4.17 Steady side view flow photos taken at the cross plane $\theta = 0°$ at H=20.0 mm for Ra=15,030 (ΔT =20.0℃) and Re_j= 811 (Q_j= 6.0 slpm) for rotational Reynolds number Re_Ω = (a)0, (b)778, (c)1,557, and (d)2,335.